NANO LETTERS

Letter

pubs.acs.org/NanoLett

Engineering Empty Space between Si Nanoparticles for Lithium-Ion Battery Anodes

Hui Wu,[†] Guangyuan Zheng,[‡] Nian Liu,[§] Thomas J. Carney,[†] Yuan Yang,[†] and Yi Cui*[,†,∥]

[†]Department of Materials Science and Engineering; [‡]Department of Chemical Engineering; [§]Department of Chemistry, Stanford University, California 94305, United States

[∥]Stanford Institute for Materials and Energy Sciences, SLAC National Accelerator Laboratory, 2575 Sand Hill Road, Menlo Park, California 94025, United States

Supporting Information

ABSTRACT: Silicon is a promising high-capacity anode material for lithium-ion batteries yet attaining long cycle life remains a significant challenge due to pulverization of the silicon and unstable solid-electrolyte interphase (SEI) formation during the electrochemical cycles. Despite significant advances in nanostructured Si electrodes, challenges including short cycle life and scalability hinder its widespread implementation. To address these challenges, we engineered an empty space between Si nanoparticles by encapsulating them in hollow carbon tubes. The synthesis process used low-cost Si nanoparticles and electrospinning methods, both of which can be easily scaled. The empty space around the Si nanoparticles allowed the electrode to successfully overcome these problems Our anode demonstrated a high gravimetric capacity (~1000 mAh/g based on the total mass) and long cycle life (200 cycles with 90% capacity retention).

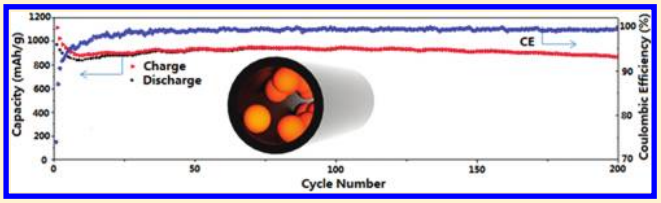

KEYWORDS: *Li-ion battery, Si anode, solid-electrolyte interphase (SEI)*

To meet the demands of future portable electronics and electric vehicles, researchers have devoted significant attention to develop high capacity electrode materials for lithium-ion batteries (Li-ion).[1,2] In particular, they have focused on conversion oxides,[1] silicon anodes,[3−7] sulfur cathodes,[8−10] and air cathodes.[11−13] Among these candidates, silicon is an exciting and promising alternative anode material to replace carbon in Li-ion batteries due to its high gravimetric capacity of ~4200 mAh/g, which is ten times higher than that of traditional graphite anode (~370 mAh/g), high volume capacity of 9786 mAh/cm^3, relatively low working potential making it suitable as an anode (~0.5 V vs Li/Li$^+$), abundance and environmentally benignity, and prevalence in the semiconductor industry and solar industry, whose techniques and expertise can aide in mass manufacturing.[14−16] However, there exist several scientific and technical challenges for silicon anodes. One challenge is the mechanical fracture caused by large volume changes. The electrochemical alloying reaction of Li with Si involves volume expansion of up to 400% during lithium insertion, and upon extraction of the lithium involves significant contraction.[3,7] The stress induced by the large volume change causes cracking and pulverization of silicon, which leads to loss of electrical contact and eventual capacity fading. Another challenge for silicon anodes is the unstable solid electrolyte interface (SEI). The repetitive volume expansion and contraction constantly shifts the interface between Si and the organic electrolyte, hence preventing the formation of a layer of stable SEI, which in turn results in a low Coulombic efficiency and a decrease in capacity during battery cycling. Moreover, silicon anodes also must maintain good electrical contact between Si materials and current collector during cycling. Even though mechanical fracture does not take place in Si nanostructures below critical sizes,[17] large volume change can still cause the movement of Si nanostructures and the detachment from the conducting environment during long-term battery cycling.[3,14,18−23] Finally, these challenges are compounded with the fact that the synthesis of these silicon anodes must be cheap and scalable to supplant current carbon anodes in Li-ion batteries.

While there has been exciting progress in addressing a subset of these challenges, few have sought to address all of these challenges simultaneously. Nanostructured Si materials afford promising opportunities to address all of these challenges because of their ability to relax strain. In addition, chemically synthesized Si nanostructures, including nanowires,[3,24] nanocrystals,[25] core−shell nanofibers,[26,27] nanotubes,[6,28] nanospheres,[29,30] nanoporous materials,[31,32] and Si/carbon nanocomposites,[5,33] have demonstrated superior performance compared to bulk Si. Moreover, the Si nanostructures have addressed the issue of separation from the current collector, resulting in significant improvements of electrochemical cycling up to hundreds of cycles. However, these studies do not have a clear indication on how to generate a static Si-electrolyte interface for stable SEI formation and the electrochemical

Received: November 10, 2011
Revised: December 14, 2011
Published: January 6, 2012

cycling performance still fails to meet the requirements for portable electronics and electric vehicles. In addition, these previously reported nanostructures involve synthesis processes such as chemical vapor deposition, complex chemical reactions, and/or templating, which are expensive and difficult to scale.

Mechanically generated Si nanoparticles from bulk polycrystalline Si are cheap, scalable, and commercially available. Numerous research groups have investigated them as candidates for Si anodes,[17,21,34−39] yet unfortunately, these reported Si electrodes still suffer from fast capacity decay. None of these nanoparticle electrodes demonstrate more than 50 cycles without significant capacity loss. Recent studies using novel polymer binders in conjunction with Si nanoparticles demonstrated potential due to the strong mechanical and conducting properties of the binders,[38−42] although they did not address how to stabilize the SEI with repetitive volume expansion and contraction. In this Letter, we combined Si nanoparticles derived from bulk Si and electrospinning to fabricate hollow carbon fiber encapsulated Si nanoparticles with an engineered hollow space between the nanoparticles and the carbon fiber wall to allow for volume expansion. We demonstrated that these structures addressed all the challenges related to Si anodes outlined above and report more than 90% capacity retention after 200 deep cycles.

Conformal conducting carbon coating on Si nanoparticles to enhance the electron conductivity of silicon nanoparticles and hence electrochemical performance has been previously reported.[43,44] However, this design still possesses three flaws. First, it does not consider the volume changes of silicon during electrochemical reactions. In particular, after lithiation, the conducting coating layers disintegrate due to the large volume expansion of silicon. As a result, these unstable coatings lose contact with one another during cycling, as schematically shown in Figure 1a. Second, the coating layer on each silicon

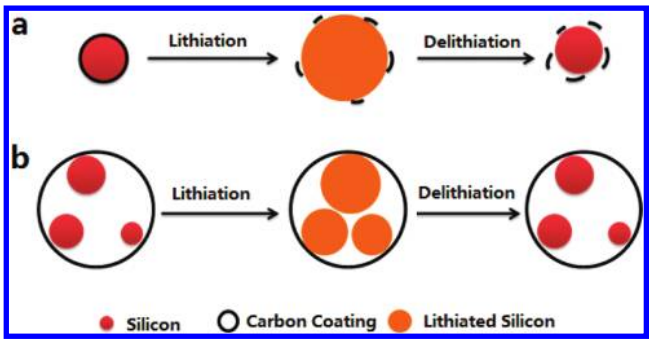

Figure 1. Schematic presentation of the materials design. (a) A conformal carbon coating on silicon nanoparticles will disintegrate due to the large volume changes experienced by Si nanoparticles during electrochemical reactions. (b) The carbon coating can be stabilized by designing an empty space inside the coating layer. The empty space allows for the free expansion and contraction of Si nanoparticles during lithiation and delithiation without any mechanical constrain or tension imposed on the Si nanoparticles. Thus, the empty space prevents damage to the carbon layer during Si volume changes.

particle is not directly in contact with the current collector, and thus junction resistances between particles cannot be avoided. Third, this electrode structure cannot prevent continuous formation of SEI on silicon.

Taking these shortcomings into consideration, we designed an anode structure with Si nanoparticles encapsulated in continuous hollow carbon tubes (SiNP@CT) to improve the electrode performance (Figure 1b). The thin carbon layers enhanced the electrical conductivity of electrode without preventing lithium ion transfer to silicon particles. The ample empty space inside the hollow tubes allowed for silicon expansion during electrochemical cycling, as schematically shown in Figure 1b. Moreover, each carbon tube was directly connected to the current collector and acted as a fast and stable electron transfer channel, supporting a stable cycling of the entire electrode as well as high charge and discharge rates. Also, this design effectively prevented SEI growth.

To synthesize the anode structure as shown in Figure 1b, we developed a low-cost and scalable synthesis method. The process flow is described in Figure 2a (see Experimental details in Supporting Information). First, Si nanoparticles were mixed with inexpensive silicon dioxide precursor solution (tetraethoxysilane (TEOS)). Next, electrospinning, a well-known, low-cost, scalable manufacturing process used widely in fiber and textile industries[45] was used to generate continuous silicon dioxide nanofibers with embedded Si nanoparticles. Recently, this technique was developed to synthesize all types of nanofibers including polymer, oxide, metal, and carbon.[45,46] Third, a thin layer of carbon was coated onto the composite nanofibers by thermal carbonization of polystyrene. The carbon-coated fibers were etched in HF aqueous solution to remove SiO_2 and leave Si. Because of the carbon layer's thinness and small yet numerous pores, the HF solution easily diffused into the fibers. Thus, a structure with Si nanoparticles encapsulated inside continuous hollow carbon tubes with adequate empty space for volume expansion was synthesized. Figure S1 in Supporting Information shows a scanning electron microscopy (SEM) image of carbon-coated Si nanoparticle/SiO_2 composite nanofibers. Figure 2b,c shows SEM and transmission electron microscopy (TEM) images of the fabricated SiNP@CT electrodes. It is apparent from these figures that after etching the SiO_2 nanofibers all the Si nanoparticles remain inside the carbon tubes, which have a side wall thickness of 7−10 nm. These continuous carbon tubes help the electrical conductivity and prevent the direct contact of Si and the electrolyte during electrochemical cycling. It is important to note that the ample empty space surrounding each Si nanoparticle allows for the free expansion of Si without mechanical constrain during lithiation and also prevents damage to the carbon layer from Si volume changes. Selected area electron diffraction (SAED) demonstrated that each Si nanoparticle is single crystalline (Figure 2c). The composition was further confirmed by energy dispersive spectroscopy (EDS) microanalysis. As shown in Figure 2d, strong signals of carbon and silicon signal were detected, and the oxygen signal was relatively low, indicating complete removal of the SiO_2 core.

Next, the electrochemical properties of the Si nanoparticle anodes were evaluated using deep galvanostatic charge/discharge cycles from 1 to 0.01 V, which would generate the capacity of pure Si ∼ 4000 mAh/g[3]. All the specific capacity values in this paper are reported using the total mass of SiNP@CT, except at the places noted. As seen in Figure 3a, the first cycle specific reversible lithium extraction capacity of the SiNP@CT structure including all the Si and carbon mass was 969 mAh/g at a charge/discharge current density of 1 A/g (defined as 1 C here), which is 3 times higher than that of traditional graphitic anodes (∼370 mAh/g). Considering the silicon mass was only 47% of the total mass of electrode, the gravimetric capacity of silicon alone is actually higher, ∼2061 mAh/g. The SiNP@CT electrode showed superior cycling

dx.doi.org/10.1021/nl203967r | Nano Lett. 2012, 12, 904−909

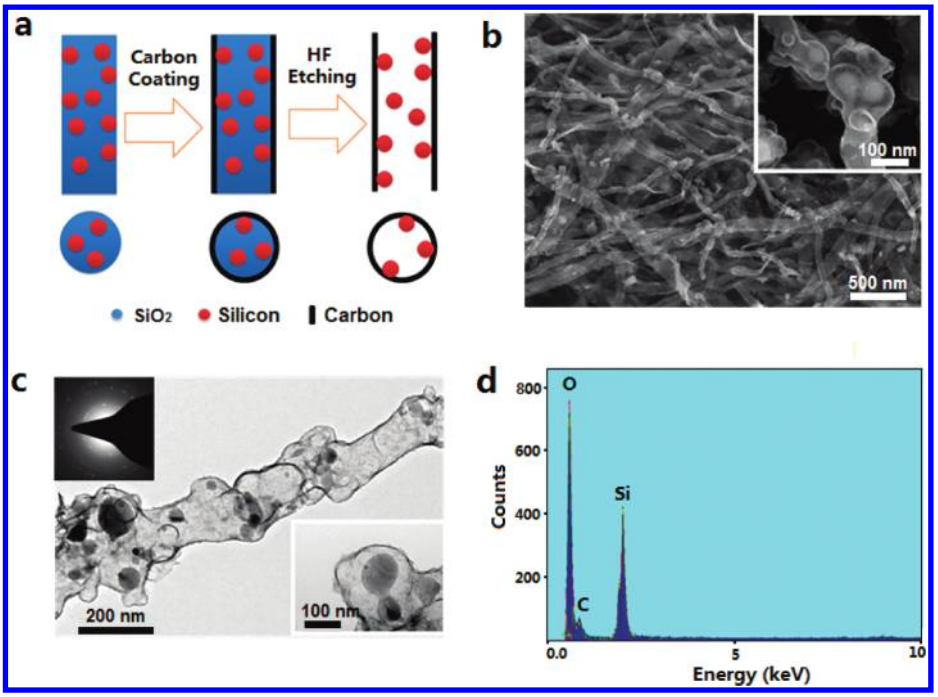

Figure 2. Fabrication and characterization. (a) Schematic outlining the material fabrication process. Si nanoparticles in SiO_2 nanofibers were first prepared by electrospinning. After carbon coating and removal of SiO_2 core, the SiNP@CT structure was obtained. (b) SEM images of synthesized SiNP@CT. (c) TEM images of synthesized samples. Lower inset shows TEM image with higher magnification; upper inset shows SAED pattern of the sample. (d) EDS spectrum of synthesized SiNP@CT samples.

stability and the discharge capacity retention after 50, 100, and 200 cycles was 95, 95, and 90%, respectively. The cycling performance of three different Si nanoparticle electrodes: bare Si nanoparticles, Si nanoparticles with carbon coating, and Si nanoparticles encapsulated in hollow carbon tubes was compared using the same charge/discharge cycling with current density (1 A/g, Figure 3b). Under the deep charge/discharge condition, a fast capacity fading for anodes made from bare silicon nanoparticles was observed and <20% of initial capacity remained after 10 cycles. By coating a carbon layer on Si nanoparticles, the cycling stability showed minimal improvements due to the enhanced electrical conductivity. However, more than half of its initial capacity was lost in 50 cycles. In comparison, SiNP@CT demonstrated a stable cycling performance. In fact, there was almost no capacity decay after 50 cycles. As seen in the voltage profiles of different cycles (Figure 3c), the lithiation potential of first cycle showed a plateau profile at 0.1−0.01 V, consistent with the behavior of crystalline Si. No obvious change in charge/discharge profile can be found after 200 cycles for Si nanoparticle encapsulated in carbon tube anode, indicating superior and stable cycling performance. As a comparison, voltage profiles of silicon nanoparticles without a stabilizing design changed after cycling (Figure 3d). Coulombic efficiency (CE) is another important consideration for silicon as anode material. In addition, the first cycle CE (71%) of the SiNP@CT was not as high as expected since the coating carbon layer is relatively low quality and the initial SEI formation consumes some of the electrolyte. The CE can be improved by prelithiation and graphitization of carbon tube in future studies.[47] As shown in Figure 3a, a high CE of >99% was achieved in the following cycles due to the stable SEI formed outside carbon tubes. In addition, the continuous carbon tubes, which are directly connected to the current collector, provided fast channels for electron transfer, and therefore enabled outstanding high power rate capability. At high charge/discharge current densities ranging from 0.8 to 8 A/g (with charge and discharge rates from 1.5 h to 10 min, respectively), high and stable capacities of 1000 to 700 mAh/g in the electrodes were demonstrated (Figure 3e,f). Clearly, Li ions rapidly passed through the thin carbon layer and reached the silicon active material even at very high C rates, and as a result the capacity decreased slightly while increasing current density. For example, we noticed a capacity drop of only 10% as the current density tripled from 0.8 to 2.4 A/g (Figure 3f). The SNP@CT electrodes also showed excellent cycle stability under high current density. In the sample shown in Figure 3e, the capacity retention was 78% after 300 cycles under various high current densities.

The superior electrochemical performance of SiNP@CT electrode is due to the stable coating layer and the stable SEI layer. As can be seen in the TEM and SEM images (Figure 2b,c), the composite electrode contained plenty of empty spaces around each Si nanoparticle, allowing it to expand freely without mechanical constrain during lithiation. Therefore, the empty space design effectively prevented damage to the carbon layer due to Si volume changes. This phenomenon was confirmed by inspecting the electrode microstructure after cycling. We disassembled the electrode after 200 electrochemical cycles and washed the electrode with acetonitrile and diluted HCl solution to remove the SEI layer. As shown in the SEM images in Figure 4c and TEM images in Figure 4d, the carbon tubes remained continuous and unbroken after cycles. The Si nanoparticles became amorphous after electrochemical reactions, as demonstrated by SAED pattern in Figure 4e. This experiment result agrees with Mai's in situ Raman study on single silicon nanowires, which showing crystalline Si lost its order and became metastable amorphous Li_xSi alloy after lithiation.[48] From Figure 4c,d, we can directly observe that Si

dx.doi.org/10.1021/nl203967r | Nano Lett. 2012, 12, 904−909

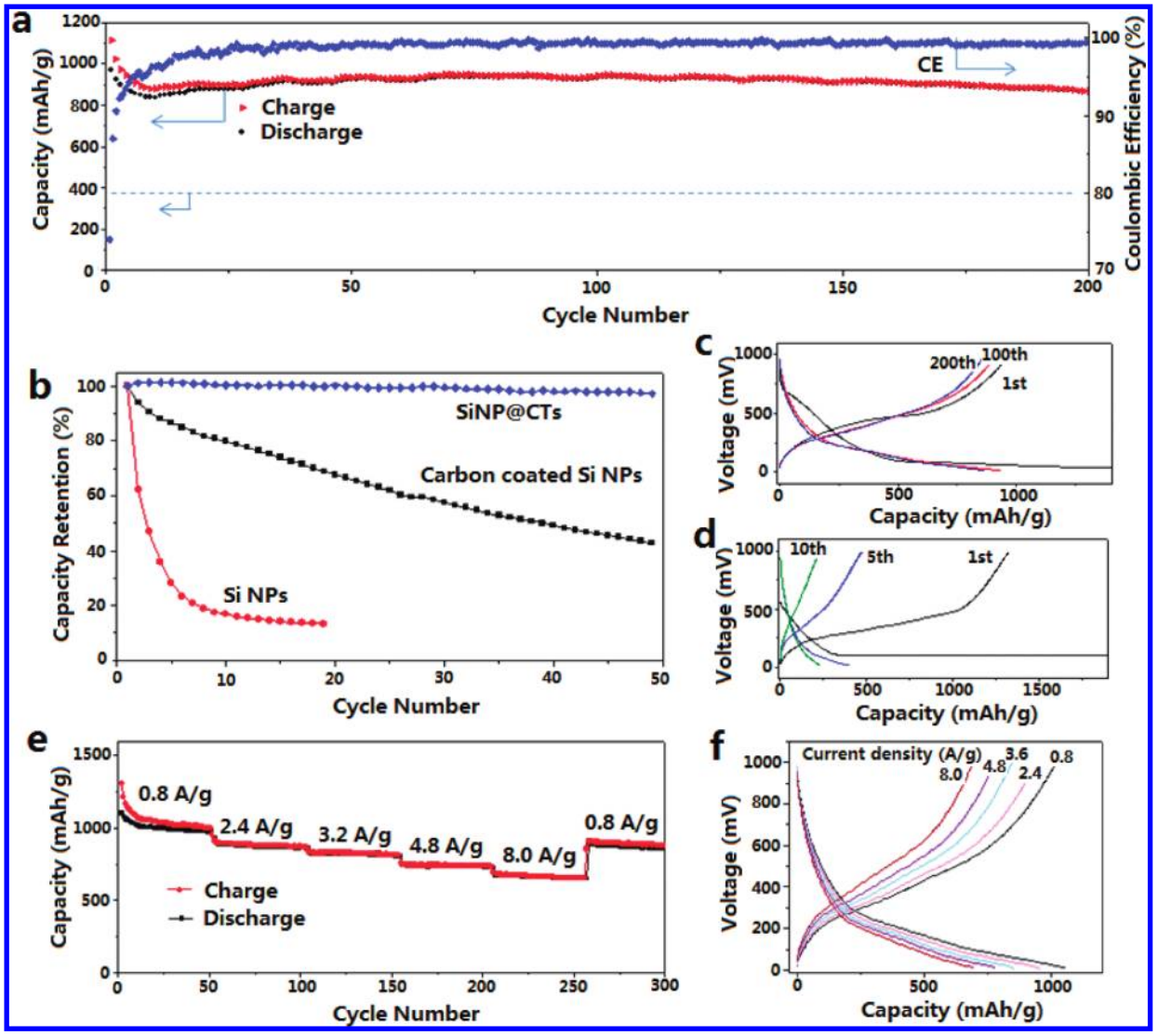

Figure 3. Electrochemical characterizations of the synthesized SiNP@CT. (a) Charge−discharge cycling test of SiNP@CT electrodes at a current density of 1A/g, showing 10% loss after 200 cycles. Dashed line indicates the theoretical capacity of traditional graphite anode. (b) Capacity retention of different Si nanostructures. (c,d) Galvanostatic charge−discharge cyclic curves of the first and later cycles of different Si nanoparticle based electrodes: (c) SiNP@CT electrode and (d) bare Si nanoparticle electrode. (e,f) Capacity retention (e) and galvanostatic charge/discharge profiles (f) of the SiNP@CT electrode cycled at various current densities ranging from 0.8 to 8 A/g. All electrochemical measurements (a−f) were carried out at room temperature in two-electrode 2032 coin-type half-cells. Capacity is calculated based on the weight of total mass.

nanoparticles remain structurally intact and in contact with the carbon tubes after electrochemical reactions, giving a stable electrochemical cycle performance. It is worth mentioning that the Li-ion capacity of bare Si nanoparticle electrode may decease through self-aggregation of nanoparticles (Figure 3d). In our SiNP@CT electrode, such particle self-aggregation has been greatly reduced since the Si nanoparticles are trapped inside carbon tubes and firmly attached to the carbon side walls, as can be demonstrated from SEM images of electrode after electrochemical cycles (Figure 4c). There are literature reports suggesting that the reduced particle self-aggregation provides a potential benefit for stable electrochemical cycles of materials.[46,49,50]

Another important advantage of this design is the formation of a stable SEI layer on the material. SEI stability is a critical factor for obtaining long cycle life although it has not been effectively addressed for materials with large volume change. The reasons are indicated in the schematic drawing in Figure 4a. Electrolyte decomposition due to the low potential of electrodes forms a self-passivated SEI layer on electrode surface. The SEI layer is an electron insulator but also a lithium ion conductor that halts the decomposition of electrolyte while maintaining the lithium ion diffusion.[23] Si nanoparticles expand upon lithiation and contract during delithiation. The SEI formed at the lithiated and expanded state can be broken at the delithiated and shrunken state. This exposes a fresh Si surface to the electrolyte and the SEI formation occurs again. Thus, charge and discharge cycling results in thicker and thicker SEI. The consumption of the electrolyte and lithium ions during SEI formation, the electrically insulating nature of SEI, the long lithium diffusion distance through thick SEI, and the electrode pulverization caused by the mechanical stress imposed by the continuous growth of SEI can result in capacity fading during cycling. In our design, silicon nanoparticles are not directly in contact with the electrolyte. If there are any pinholes in the carbon hollow tube walls and some electrolyte leakage, they can

dx.doi.org/10.1021/nl203967r | Nano Lett. 2012, 12, 904−909

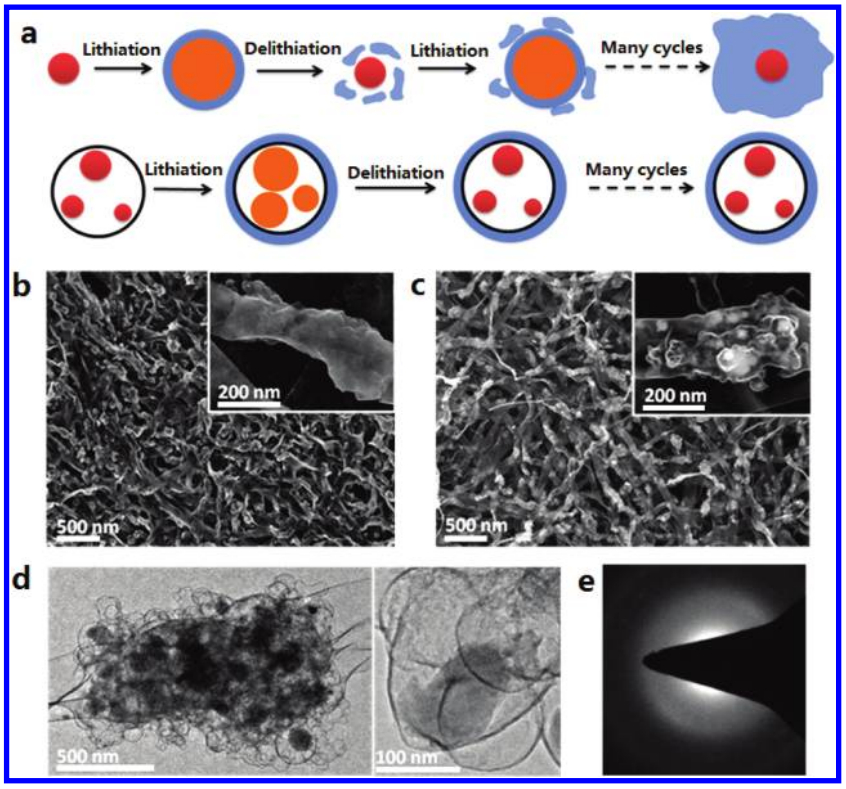

Figure 4. Material morphology after electrochemical cycles. (a) Schematic of SEI formation on Si nanoparticles without and with our presented carbon coatings. (b) SEM image of SiNP@CT electrode after 200 electrochemical samples. A thin layer of SEI can be observed outside tubes. (c–e) SEM images (c), TEM images, (d) and SAED pattern (e) of the same cycled SiNP@CT electrode after dissolving the SEI layer by HCl washing.

be sealed by decomposition of small amount of electrolyte. Thus, almost all the SEI can be considered to be only on the outside of the carbon tubes. Since the empty space inside tubes provides adequate space for Si expansion, there are no changes of the interface between electrode and electrolyte. As a result, stable SEI can be retained during cycling. In Figure 4b, we observed a thin and uniform SEI layer after 200 cycles. As a comparison, for the Si nanoparticle electrode after electrochemical cycling, we noticed a thick SEI layer coating the entire electrode, indicating the continuous growth of SEI (Supporting Information Figure S2). The stable SEI formed outside SiNP@CT also helped to achieve a high CE of >99%.

In summary, we designed and fabricated Si nanoparticle-based electrodes by addressing the three main challenges for Si electrodes: mechanical instability, current collector contact, and unstable SEI. By encapsulating Si nanoparticle in a carbon tube structure, we successfully addressed these problems and achieved high cycle stability (90% capacity retention after 200 cycles). The entire fabrication process is scalable and does not involve expensive silicon growth steps.

■ ASSOCIATED CONTENT

Ⓢ Supporting Information

Experimental details. SEM images of synthesized nanofibers and SEI formation on Si nanoparticles. This material is available free of charge via the Internet at http://pubs.acs.org.

■ AUTHOR INFORMATION

Corresponding Author

*E-mail: yicui@stanford.edu.

■ ACKNOWLEDGMENTS

This work was partially supported by the Assistant Secretary for Energy Efficiency and Renewable Energy, Office of Vehicle Technologies of the U.S. Department of Energy, under Contract No. DE-AC02-05CH11231, Subcontract No. 6951379 under the Batteries for Advanced Transportation Technologies (BATT) Program. A portion of this work was supported by the Department of Energy, Office of Basic Energy Sciences, Division of Materials Sciences and Engineering under contract DE-AC02-76SF00515 through the SLAC National Accelerator Laboratory LDRD project.

■ REFERENCES

(1) Tarascon, J. M.; Armand, M. *Nature* **2001**, *414*, 359–367.
(2) Bruce, P. G.; Scrosati, B.; Tarascon, J. M. *Angew. Chem., Int. Ed.* **2008**, *47*, 2930–2946.
(3) Chan, C. K.; Peng, H. L.; Liu, G.; McIlwrath, K.; Zhang, X. F.; Huggins, R. A.; Cui, Y. *Nat. Nanotechnol.* **2008**, *3*, 31–35.
(4) Esmanski, A.; Ozin, G. A. *Adv. Funct. Mater.* **2009**, *19*, 1999–2010.
(5) Magasinski, A.; Dixon, P.; Hertzberg, B.; Kvit, A.; Ayala, J.; Yushin, G. *Nat. Mater.* **2010**, *9*, 353–358.
(6) Park, M. H.; Kim, M. G.; Joo, J.; Kim, K.; Kim, J.; Ahn, S.; Cui, Y.; Cho, J. *Nano Lett.* **2009**, *9*, 3844–3847.
(7) Hatchard, T. D.; Dahn, J. R. *J. Electrochem. Soc.* **2004**, *151*, A838–A842.
(8) Ji, X. L.; Lee, K. T.; Nazar, L. F. *Nat. Mater.* **2009**, *8*, 500–506.
(9) Yang, Y.; McDowell, M. T.; Jackson, A.; Cha, J. J.; Hong, S. S.; Cui, Y. *Nano Lett.* **2010**, *10*, 1486–1491.
(10) Jayaprakash, N.; Shen, J.; Moganty, S. S.; Corona, A.; Archer, L. A. *Angew. Chem., Int. Ed.* **2011**, *50*, 5904–5908.
(11) Debart, A.; Paterson, A. J.; Bao, J.; Bruce, P. G. *Angew. Chem., Int. Ed.* **2008**, *47*, 4521–4524.

(12) Mitchell, R. R.; Gallant, B. M.; Thompson, C. V.; Shao-Horn, Y. *Energy Environ. Sci.* **2011**, *4*, 2952−2958.
(13) Xiao, J.; Mei, D. H.; Li, X. L.; Xu, W.; Wang, D. Y.; Graff, G. L.; Bennett, W. D.; Nie, Z. M.; Saraf, L. V.; Aksay, I. A.; Liu, J.; Zhan, J. G. *Nano Lett.* **2011**, *11*, 5071.
(14) Park, C. M.; Kim, J. H.; Kim, H.; Sohn, H. J. *Chem. Soc. Rev.* **2010**, *39*, 3115−3141.
(15) Szczech, J. R.; Jin, S. *Energy Environ. Sci.* **2011**, *4*, 56−72.
(16) Zhang, W. J. *J. Power Sources* **2011**, *196*, 13−24.
(17) Kim, H.; Seo, M.; Park, M. H.; Cho, J. *Angew. Chem., Int. Ed.* **2010**, *49*, 2146−2149.
(18) Choi, N. S.; Yao, Y.; Cui, Y.; Cho, J. *J. Mater. Chem.* **2011**, *21*, 9825−9840.
(19) Hertzberg, B.; Alexeev, A.; Yushin, G. *J. Am. Chem. Soc.* **2010**, *132*, 8548−.
(20) Kamali, A. R.; Fray, D. J. *J. New Mater. Electrochem. Syst.* **2010**, *13*, 147−160.
(21) Ryu, J. H.; Kim, J. W.; Sung, Y. E.; Oh, S. M. *Electrochem. Solid State Lett.* **2004**, *7*, A306−A309.
(22) Beaulieu, L. Y.; Eberman, K. W.; Turner, R. L.; Krause, L. J.; Dahn, J. R. *Electrochem. Solid State Lett.* **2001**, *4*, A137−A140.
(23) Chan, C. K.; Ruffo, R.; Hong, S. S.; Cui, Y. *J. Power Sources* **2009**, *189*, 1132−1140.
(24) Huang, R.; Fan, X.; Shen, W. C.; Zhu, J. *Appl. Phys. Lett.* **2009**, 95.
(25) Kim, H.; Seo, M.; Park, M. H.; Cho, J. *Angew. Chem., Int. Ed.* **2010**, *49*, 2146−2149.
(26) Cui, L. F.; Ruffo, R.; Chan, C. K.; Peng, H. L.; Cui, Y. *Nano Lett.* **2009**, *9*, 491−495.
(27) Cui, L. F.; Yang, Y.; Hsu, C. M.; Cui, Y. *Nano Lett.* **2009**, *9*, 3370−3374.
(28) Song, T.; Xia, J. L.; Lee, J. H.; Lee, D. H.; Kwon, M. S.; Choi, J. M.; Wu, J.; Doo, S. K.; Chang, H.; Il Park, W.; Zang, D. S.; Kim, H.; Huang, Y. G.; Hwang, K. C.; Rogers, J. A.; Paik, U. *Nano Lett.* **2010**, *10*, 1710−1716.
(29) Ma, H.; Cheng, F. Y.; Chen, J.; Zhao, J. Z.; Li, C. S.; Tao, Z. L.; Liang, J. *Adv. Mater.* **2007**, *19*, 4067−.
(30) Yao, Y.; McDowell, M. T.; Ryu, I.; Wu, H.; Liu, N. A.; Hu, L. B.; Nix, W. D.; Cui, Y. *Nano Lett.* **2011**, *11*, 2949−2954.
(31) Teki, R.; Datta, M. K.; Krishnan, R.; Parker, T. C.; Lu, T. M.; Kumta, P. N.; Koratkar, N. *Small* **2009**, *5*, 2236−2242.
(32) Kim, H.; Han, B.; Choo, J.; Cho, J. *Angew. Chem., Int. Ed.* **2008**, *47*, 10151−10154.
(33) Magasinski, A.; Dixon, P.; Hertzberg, B.; Kvit, A.; Ayala, J.; Yushin, G. *Nat. Mater.* **2010**, *9*, 353−358.
(34) Zhang, T.; Gao, J.; Fu, L. J.; Yang, L. C.; Wu, Y. P.; Wu, H. Q. *J. Mater. Chem.* **2007**, *17*, 1321−1325.
(35) Ji, L. W.; Zhang, X. W. *Carbon* **2009**, *47*, 3219−3226.
(36) Lee, J. K.; Smith, K. B.; Hayner, C. M.; Kung, H. H. *Chem. Commun.* **2010**, *46*, 2025−2027.
(37) Liu, Y.; Wen, Z. Y.; Wang, X. Y.; Yang, X. L.; Hirano, A.; Imanishi, N.; Takeda, Y. *J. Power Sources* **2009**, *189*, 480−484.
(38) Li, J.; Le, D. B.; Ferguson, P. P.; Dahn, J. R. *Electrochim. Acta* **2010**, *55*, 2991−2995.
(39) Li, J.; Lewis, R. B.; Dahn, J. R. *Electrochem. Solid State Lett.* **2007**, *10*, A17−A20.
(40) Kovalenko, I.; Zdyrko, B.; Magasinski, A.; Hertzberg, B.; Milicev, Z.; Burtovyy, R.; Luzinov, I.; Yushin, G. *Science* **2011**, *333*, 75−79.
(41) Chen, Y. H.; Wang, C. W.; Liu, G.; Song, X. Y.; Battaglia, V. S.; Sastry, A. M. *J. Electrochem. Soc.* **2007**, *154*, A978−A986.
(42) Liu, G.; Xun, S. D.; Vukmirovic, N.; Song, X. Y.; Olalde-Velasco, P.; Zheng, H. H.; Battaglia, V. S.; Wang, L. W.; Yang, W. L. *Adv. Mater.* **2011**, *23*, 4679.
(43) Dimov, N.; Kugino, S.; Yoshio, M. *Electrochim. Acta* **2003**, *48*, 1579−1587.
(44) Yoshio, M.; Wang, H. Y.; Fukuda, K.; Umeno, T.; Dimov, N.; Ogumi, Z. *J. Electrochem. Soc.* **2002**, *149*, A1598−A1603.
(45) Li, D.; Xia, Y. N. *Adv. Mater.* **2004**, *16*, 1151−1170.
(46) Mai, L. Q.; Xu, L.; Han, C. H.; Luo, Y. Z.; Zhao, S. Y.; Zhao, Y. L. *Nano Lett.* **2010**, *10*, 4750−4755.
(47) Lee, J. K.; An, K. W.; Ju, J. B.; Cho, B. W.; Cho, W. I.; Park, D.; Yun, K. S. *Carbon* **2001**, *39*, 1299−1305.
(48) Mai, L. Q.; Dong, Y. J.; Xu, L.; Han, C. H. *Nano Lett.* **2010**, *10*, 4273−4278.
(49) Liu, J. P.; Jiang, J.; Cheng, C. W.; Li, H. X.; Zhang, J. X.; Gong, H.; Fan, H. J. *Adv. Mater.* **2011**, *23*, 2076−.
(50) Mai, L. Q.; Yang, F.; Zhao, Y. L.; Xu, X.; Xu, L.; Luo, Y. Z. *Nat. Commun.* **2011**, *2*, 381.